British Journal of Pharmacology

DOI:10.1111/j.1476-5381.2011.01692.x
www.brjpharmacol.org

RESEARCH PAPER

A novel compound PTIQ protects the nigral dopaminergic neurones in an animal model of Parkinson's disease induced by MPTP

Hyo Jin Son[1], Ji Ae Lee[1], Nari Shin[1], Ji Hyun Choi[1], Jai Woong Seo[3], Dae Yoon Chi[3,4], Cheol Soon Lee[5], Eun-Mee Kim[1,6], Han Choe[2] and Onyou Hwang[1]

Departments of [1]Biochemistry and Molecular Biology and [2]Physiology, University of Ulsan College of Medicine, Seoul, [3]Department of Chemistry, Inha University, Incheon, [4]Sogang University, Seoul, [5]R&D Institute of Egene, Incheon, and [6]Department of Emergency Medical Technology, Korea Nazarene University, Cheonan, Korea

Correspondence
Onyou Hwang, Department of Biochemistry and Molecular Biology, University of Ulsan College of Medicine, 388-1 Pungnap-dong, Songpa-ku, Seoul 138-736, Korea. E-mail: oyhwang@amc.seoul.kr or Dae Yoon Chi, Department of Chemistry, Sogang University, Seoul 121-742, Korea. E-mail dychi@sogang.ac.kr

Keywords
dopaminergic neuron; MMP-3; microglia; MPTP; Parkinson's disease; pharmacokinetics

Received
20 October 2010
Revised
10 August 2011
Accepted
12 September 2011

BACKGROUND AND PURPOSE

In Parkinson's disease, the dopaminergic neurones in the substantia nigra undergo degeneration. While the exact mechanism for the degeneration is not completely understood, neuronal apoptosis and neuroinflammation are thought to be key contributors. We have recently established that MMP-3 plays crucial roles in dopaminergic cell death and microglial activation.

EXPERIMENTAL APPROACH

We tested the effects of 7-hydroxy-6-methoxy-2-propionyl-1,2,3,4-tetrahydroisoquinoline (PTIQ) on expression of MMP-3 and inflammatory molecules and dopaminergic cell death *in vitro* and in an animal model of Parkinson's disease, and Parkinson's disease-related motor deficits. The pharmacokinetic profile of PTIQ was also evaluated.

KEY RESULTS

PTIQ effectively suppressed the production of MMP-3 induced in response to cellular stress in the dopaminergic CATH.a cell line and prevented the resulting cell death. In BV-2 microglial cells activated with lipopolysaccharide, PTIQ down-regulated expression of MMP-3 along with IL-1β, TNF-α and cyclooxygenase-2 and blocked nuclear translocation of NF-κB. In the mouse model of Parkinson's disease ,induced by 1-methyl-4-phenyl-1,2,3,6-tetrahydropyridine (MPTP), PTIQ attenuated the associated motor deficits, prevented neurodegeneration and suppressed microglial activation in the substantia nigra. Pharmacokinetic analysis showed it was relatively stable against liver microsomal enzymes, did not inhibit the cytochrome p450 isozymes or the hERG ion channel, exhibited no cytotoxicity on liver cells or lethality when administered at 1000 mg kg^{-1} and entered the brain rather rapidly yielding a 28% brain:plasma ratio after i.p. injection.

CONCLUSIONS AND IMPLICATIONS

These results suggest PTIQ has potential as a candidate drug for disease-modifying therapy for Parkinson's disease.

Abbreviations

β2M, β2-microglobulin; BH4, tetrahydrobiopterin; COX-2, cyclooxygenase-2; CYP, cytochrome P450; FBS, fetal bovine serum; hERG, human ether-à-go-go related gene; LDH, lactate dehydrogenase; LPS, lipopolysaccharide; MMP, matrix metalloproteinase; MPTP, 1-methyl-4-phenyl-1,2,3,6-tetrahydropyridine; PCR, polymerase chain reaction; PMSF, phenyl methanesulphonyl fluoride; PTIQ, 7-hydroxy-6-methoxy-2-propionyl-1,2,3,4-tetrahydroisoquinoline; RT, reverse transcription; SN, substantia nigra; TH, tyrosine hydroxylase

Introduction

Parkinson's disease is the second most common neurodegenerative disease and is accompanied by motor deficits including tremor, rigidity, postural imbalance and bradykinesia. In Parkinson's disease, the dopaminergic neurones in the substantia nigra (SN) pars compacta undergo degeneration, resulting in the characteristic symptoms. The current treatment for Parkinson's disease involves administration of drugs that facilitate dopaminergic neurotransmission such as the dopamine precursor L-DOPA and deep brain stimulation following surgical manipulation. None of the currently available therapies, however, can delay the degeneration itself, and therefore ways to modify the disease course by neuroprotection are much needed.

While the mechanism by which the degeneration occurs is not completely understood, both neuronal apoptosis and inflammation are thought to play roles. Because the nigral dopaminergic neurones are particularly vulnerable, various cellular stresses can cause activation of a cascade of events leading to apoptotic death (Hurelbrink *et al.*, 2001; Tatton *et al.*, 2003). In addition, neuroinflammation involving activated microglia is thought to contribute to the chronic and progressive nature of the degeneration (Gao *et al.*, 2003; Hald and Lotharius, 2005; Tansey *et al.*, 2007; Hirsch and Hunot, 2009).

MMP-3, a member of the MMP family of proteases involved in degradation and remodelling of the extracellular matrix (Visse and Nagase, 2003), has been recently reported to have an additional role in dopaminergic neurodegeneration. Thus, MMP-3 participated in apoptotic signalling and this was reversed by pharmacological inhibition, gene knockdown and gene knockout of MMP-3 *in vitro* (Choi *et al.*, 2008; Kim *et al.*, 2010a). In addition, MMP-3 is released from dying dopaminergic cells (Kim *et al.*, 2005b; Choi *et al.*, 2008) and causes activation of microglia (Kim *et al.*, 2005b, 2007). Furthermore, MMP-3 produced inside the activated microglia mediates generation of proinflammatory molecules (Mun-Bryce *et al.*, 2002; Nuttall *et al.*, 2007; Woo *et al.*, 2008). Taken together, modulation of MMP-3 may prevent neurodegeneration via suppression of neuroinflammatory responses as well as direct neuroprotection (Kim and Hwang, 2011). As such, tissue inhibitor of metalloproteinase-1, the endogenous inhibitor of MMP-3, provides neuroprotection against cell stress in dopaminergic cells when over-expressed (Kim *et al.*, 2010a) and in primary neuronal cultures and mouse model of traumatic and ischaemic brain injury (Tejima *et al.*, 2009). Doxycycline, a tetracycline derivative, can suppress the induction of MMP-3 and protect dopaminergic neurones both *in vitro* and *in vivo* (Cho *et al.*, 2009). In addition, MMP-3 gene knockout resulted in protection of the nigral dopaminergic neurones in the mouse model of Parkinson's disease induced by 1-methyl-4-phenyl-1,2,3,6-tetrahydropyridine (MPTP) (Kim *et al.*, 2007).

In the present study, we report that a novel synthetic compound, 7-hydroxy-6-methoxy-2-propionyl-1,2,3,4-tetrahydroisoquinoline (PTIQ), down-regulated the induction of MMP-3 in both stressed dopaminergic cells and activated microglia, and provided neuroprotection of the nigral dopaminergic neurones in MPTP-treated animals.

Methods

Synthesis and structural analysis of PTIQ

To a solution of 3-*O*-methyldopamine hydrochloride (1.0 g, 4.91 mmol) in 1 M HCl was added 36% formaldehyde (2.5 mL) under N_2 atmosphere and heated at 70°C for 1 h. The solvent was evaporated under reduced pressure. The residue was crystallized in ethanol-ether to yield 7-hydroxy-6-methoxy-1,2,3,4-tetrahydroisoquinoline hydrochloride as a pale yellow solid (0.74 g, 70%): ^{1}H NMR (DMSO-d_6, 200 MHz) 9.39 (br, 2H), 9.08 (br, 1H), 6.75 (s, 1H), 6.60 (s, 1H), 4.07 (brs, 2H), 3.74 (s, 3H), 3.27–3.30 (brm, 2H), 2.88 (t, J = 9.8 Hz, 2H); ^{13}C NMR (DMSO-d_6, 50 MHz) 146.7, 145.2, 128.6, 125.6, 113.7, 113.3, 56.4, 47.7, 44.1, 28.7. CAS no. 1078–26-8.

To a solution of 7-hydroxy-6-methoxy-1,2,3,4-tetrahydroisoquinoline hydrochloride (2.0 mmol, 420 mg) in CH_2Cl_2 (10 mL), propionic anhydride (3.2 mmol, 410 mg) and triethylamine (1 mL) were added at room temperature. The mixture was stirred for 1 h and then quenched with H_2O. After extraction with CH_2Cl_2, the organic layer was dried over anhydrous sodium sulphate. After filtration, the solvent was evaporated. The resulting crude mixture (0.25 g) was dissolved in methanol, and potassium carbonate (370 mg) was added. The reaction was refluxed for 2 h. After cooling down, the mixture was extracted with dichloromethane, and the organic layer was washed with 1 M HCl solution and brine. The solution was then concentrated, and fresh-column chromatography yielded PTIQ (Figure 1; 216 mg, 91%) as a white solid: ^{1}H NMR ($CDCl_3$, 200 MHz) δ 6.72 (s, one conformer of C5-H or C8-H), 6.66 (s, one conformer of C5-H or C8-H), 6.62 (s, one conformer of C5-H or C8-H), 6.60 (s, one conformer of C5-H or C8-H), 6.10 (s, one conformer of O-H), 5.96 (s, one conformer of O-H), 4.62 (s, one conformer of C-1), 4.50 (s, one conformer of C-1), 3.86 (s, one conformer of O-CH_3), 3.83 (s, 3H, O-CH_3), 3.80 (t, J = 5.8 Hz, conformer of C-4), 3.64 (t, J = 5.8 Hz, conformer of C-4), 2.78 (m, 2H, C-3), 2.46 (q, J = 7.4 Hz, 2H), 1.18 (td, J = 7.4, 3.0 Hz, 3H); ^{13}C NMR ($CDCl_3$, 50 MHz) δ 172.8, 145.5, 144.6, 144.3, 126.1, 125.1, 112.5, 111.8, 111.0, 110.6, 56.0, 46.8, 43.8, 43.2, 39.8, 29.1, 28.1, 26.9, 26.7, 9.4; MS (EI) 235 (M^+, 100), 220, 178, 163, 150.

The reaction progress was followed by visualization on TLC by UV light or phosphomolybdic acid indicator. Chemical shifts were reported in parts per million and were referenced against internal solvent peaks. Coupling constants were reported in Hz. ^{1}H and ^{13}C NMR spectra were obtained on 200 MHz spectrometers (Varian, Palo Alto, CA, USA). Mass

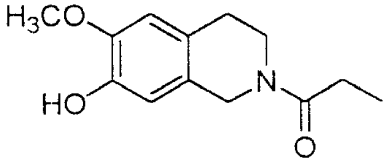

Figure 1

Chemical structure of 7-hydroxy-6-methoxy-2-propionyl-1,2,3,4-tetrahydroisoquinoline (PTIQ).

spectra were obtained from facilities at the Korea Basic Science Institute (Daegu, Korea).

Cell cultures

The CATH.a catecholaminergic cell line [provided by Dr Dona Chikaraishi (Tufts University, MA, USA); Suri *et al.*, 1993] were grown in RPMI culture medium 1640 containing 8% horse serum, 4% fetal bovine serum (FBS) and penicillin-streptomycin. They were plated at a density of 0.5×10^5 cells per·well in 96-well culture plates or 1.5×10^6 cells per·well in 6-well culture plates. The BV-2 mouse microglial cells [provided by Dr Tong Joh (Cornell University, NY, USA); Blasi *et al.*, 1990] were grown in Dulbecco's modified Eagle's medium with 10% FBS in the presence of 100 IU L^{-1} penicillin and 10 μg mL^{-1} streptomycin. For experiments, the cells were seeded on polystyrene tissue culture dishes at the following densities: 0.5×10^5 cells per·well in 96-well culture plates, 1×10^6 cells per·well in 6-well culture plates and 2.6×10^6 cells in 60 mm plates. After 24 h, the cells were fed with fresh medium and treated. All cells were maintained at 37°C in 95% air and 5% CO_2 in humidified atmosphere.

Western blot analysis

Western blot analysis was performed on total cell lysate and brain tissue homogenates. Briefly, cells were washed with ice-cold PBS and lysed on ice in RIPA buffer (25 mM Tris-HCl pH 7.5, 150 mM NaCl, 2 mM EDTA pH 8.0, 0.5% NP-40) containing protease inhibitor cocktail. Brain tissue was homogenized in ice-cold 10 mM phosphate buffer (pH 6.5) containing 0.1% NP-40 using a tissue grinder. After centrifugation at 14 000× *g* for 10 min, the supernatant was obtained. Protein concentrations were determined, and equal amounts of protein were separated on a 10% SDS polyacrylamide gel and transferred onto polyvinylidene difluoride-nitrocellulose filters. After treatment in blocking solution [6% skim milk in TTBS buffer (composition;10 mM Tris-HCl, pH 7.5, 150 mM NaCl, and 0.4% Tween-20)] for 1 h, the membrane was incubated overnight with primary antibodies (MMP-3, 1:500; COX-2, 1:200; tyrosine hydroxlyase (TH), 1:5000 [polyclonal]; NF-κB p65, 1:500; β-actin, 1:1000; lamin B, 1:500) at 4°C followed by horseradish peroxidase-conjugated secondary antibodies for 1 h at room temperature. Protein bands were detected by chemiluminescence. Densitometric analysis was performed using Image Gauge 4.0 program (Fujifilm, Tokyo, Japan), and the data were normalized against β-actin or lamin B, used as cytosolic and nuclear loading controls, respectively.

LDH activity assay

Aliquots (50 μL) of cell culture medium were incubated at room temperature in the presence of 0.26 mM NADH, 2.87 mM sodium pyruvate, and 100 mM potassium phosphate buffer (pH 7.4) in a total volume of 200 μL. The rate of NAD^+ formation was monitored for 5 min at 2 s intervals at 340 nm using a microplate spectrophotometer (SPECTRA MAX 340 pc; Molecular Devices, Menlo Park, CA, USA).

RT-PCR for MMP-3, TNF-α, IL-1β and COX-2

RT reactions were performed using 5 μg of total RNA isolated from BV-2 cells and the first strand cDNA synthesis kit following the manufacturer's directions. PCR were performed at 94°C for 30 s, 60°C for 40 s, and 72°C for 1 min for 30 cycles using the following sets of primers: MMP-3 (forward, CTTCAGTACCTTCCCAGGTTCG; reverse, CGAGGACATC AGGGGATGCTG), TNF-α (forward, CAGACCCTCACACTCA GATCATCTT; reverse, CAGAGCAATGACTCCAAAGTAGA CCT), IL-1β (forward, ATGGCAACTGTTCCTGAACTCAACT; reverse, CAGGACAGGTATAGATTCTTTCCTTT), COX-2 (forward, CAGCAAATCCTTGCTGTTCC; reverse, TGGGCAAA GAATGCAAACATC) and β2-microglobulin (β2M) (forward, GCTATCCAGAAAACCCCTCAA; reverse, CATGTCTCGATC CCAGTAGACGGT). RT-PCR against β2M was performed as an internal control. Analysis of each PCR product on 1.5% agarose gel showed a single-band with expected size. Densitometric analysis was performed using Image Gauge 4.0 program, and the data were normalized against β2M.

Measurement of TNF-α level

BV-2 cells were washed with PBS and lysed on ice in lysis buffer (50 mM Tris-HCl pH 8.0, 150 mM NaCl, 1% NP-40) containing protease inhibitor cocktail. After centrifugation at 14 000× *g* for 10 min, the supernatant was retained. After protein quantitation, 500 μg protein was subjected to TNF-α assay by ELISA according to the protocol provided by the manufacturer. The concentration of TNF-α was calculated from a standard curve.

Preparation of nuclear extract

BV-2 cells were washed with PBS, harvested in PBS by scraping and pelleted by centrifugation at 1500× *g* for 5 min. The cell pellet was resuspended in 400 μL of cold buffer containing 10 mM HEPES pH 7.9, 10 mM KCl, 0.1 mM EDTA, 0.1 mM EGTA, 1 mM dithiothreitol and 0.5 mM PMSF by gentle pipetting. The cells were allowed to swell on ice for 15 min, after which 25 μL of 10% NP-40 (0.5%) was added and mixed for 10 s. The homogenate was then centrifuged at 14 000× *g* for 30 s, the supernatant was removed and the nuclear pellet was resuspended in 50 μL of ice-cold buffer containing 20 mM HEPES pH 7.9, 400 mM NaCl, 1 mM dithiothreitol, 1 mM EDTA, 1 mM EGTA and 1 mM PMSF. The sample was mixed thoroughly and placed on a rotary shaker for 15 min. After centrifugation at 11 000× *g* for 15 min, the soluble fraction containing nuclear proteins was obtained. Samples (5μg protein) were analysed by Western blotting for NF-κB p65.

Production of the animal model of Parkinson's disease induced by MPTP

All animal care and experimental procedures complied with the USA National Institute of Health Guide for the Care and Use of Laboratory Animals (NIH Publications no. 86–23, revised 1985) and were approved by the Animal Experiment Review Committee of the Asan Institute for Life Science. All efforts were made to minimize animal suffering. Eight-week-old male C57BL/6J mice weighing 23–25 g (Orient Corp., Sungnam, Korea) were used. The animals were housed in a temperature- and humidity-controlled room with a 12 h light/dark cycle and were allowed food and water *ad libitum*. They were divided into four groups (n = 10 each): the saline-treated control, MPTP-treated, MPTP plus PTIQ-treated and PTIQ-treated. PTIQ was given i.p. at 3 or 30 mg·kg^{-1} twice at

24 h intervals. Two hours after the second PTIQ injection, MPTP (20 mg kg^{-1}) dissolved in saline was injected i.p. four times, 2 h apart.

Hindlimb test

The hindlimb test was performed at 24 h after the last injection of MPTP as previously described (Gantois *et al.*, 2007) with a minor modification in the scoring system. The animals were suspended by the tail and scored on a scale of 0–4 based on the position of their hindlimbs. Each mouse received a score of 4, from which the score of one was deducted for each abnormal hindlimb movement of the joint or limb.

Rotarod test

The rotarod test was performed using a rotarod apparatus (Ugo Basile Biological Research, Varese, Italy). Briefly, before drug administration, mice were trained on the rotarod rotating at a constant speed of 20 rpm for 150 s, three times a day for 2 days. If the mice did not stay on the rod for the full 150 s, the trials were repeated. Six days after the MPTP injection, the mice were subjected to rotarod test at a fixed speed of 30 rpm. Three consecutive trials were made at 60 min intervals. The time taken for the mouse to fall from the rod was measured.

Vertical grid test

The vertical grid test was performed as described previously (Kim *et al.*, 2010b). Before drug administration, mice were allowed to train on the apparatus, twice a day for two consecutive days: they were placed at the bottom of the apparatus facing upward so that they would climb up the apparatus and then descend. On Day 6, 60 min after the animals had been tested on the rotarod, the same vertical grid trials were made and videotaped. The videos were replayed to analyse the time taken to climb down and also to make a complete turn.

Tissue preparation for staining

The animals were killed 7 days after the first injection. They were deeply anesthetized (80 mg kg^{-1} ketamine and 20 mg kg^{-1} xylazine, injected i.p.) and transcardially fixed in 4% paraformaldehyde as described previously (Hwang *et al.*, 1998). Brains and livers were promptly removed and postfixed in 4% paraformaldehyde. After cryoprotection, the brain tissues were cut into 20 µm sections on a vibrating-blade microtome (VT 1000S; Leica, Nussloch, Germany), and the sections were stored in 0.08% sodium azide in PBS at 4°C until analysis. The liver tissues were paraffin-embedded and cut into 4 µm sections and stained with hematoxylin and eosin.

Immunohistochemistry

Immunostaining of the nigral and striatal brain tissue sections was performed as described previously (Hwang *et al.*, 1998), using polyclonal antisera against TH (1:1000) or Iba-1 (1:200), Vectastain ABC kit and biotinylated secondary antibodies. The samples were visualized by incubation in 0.05% 3,3′-diaminobenzidine and 0.003% H_2O_2. Quantitative analysis was performed using Image Gauge 4.0. To account for differences in background-staining intensity, average background density was calculated from three microscopic fields in regions lacking immunoreactive profiles, and this was subtracted from the density of TH-positive area to obtain the final immunodensity value.

Double immunofluorescence labelling against TH and Iba-1

Tissue sections were incubated with blocking solution containing 1% BSA, 0.2% Triton X-100 and 0.05% sodium azide, rinsed in 0.5% BSA in PBS twice and then incubated with anti-TH monoclonal (1:5000) and anti-Iba-1 polyclonal (1:200) antibodies for 1 h at room temperature. The sections were washed three times and incubated for 90 min with Fluor Alexa 488-labeled anti-mouse IgG (1:200) and Fluor Alexa 546-labeled anti-rabbit IgG (1:200). After washing twice, they were mounted onto gelatin-coated slides, dried at 50°C for 30 min, coverslipped with DAKO Fluorescent mounting medium, and viewed under a confocal microscope (TCS-ST2; Leica, Wetzlar, Germany).

Double fluorescence staining against FluoroJade C and TH

Double staining with FluoroJade C and anti-TH antibody was carried out as described previously (Kim *et al.*, 2005a). Tissue sections were incubated with blocking solution containing 1% BSA, 0.2% Triton X-100 and 0.05% sodium azide, rinsed in 0.5% BSA in PBS twice and then incubated with anti-TH polyclonal antibody (1:5000) for 2 h at room temperature. The sections were washed three times and incubated for 90 min with Fluor Alexa 546-labeled anti-rabbit IgG (1:200). After washing twice, they were mounted onto gelatin-coated slides and dried at 50°C for 30 min. The samples were rehydrated, incubated in 0.06% potassium permanganate solution for 6 min and then rinsed for 2 min in distilled water. The samples were then subjected to FluoroJade C (0.0001% dissolved in 0.1% acetic acid) for 10 min and rinsed. After air drying and clearing in xylene, they were coverslipped with DAKO Fluorescent mounting medium. FluoroJade C and TH were detected by confocal microscopy.

Measurement of IL-1β level

Nigral tissue was homogenized in 4-fold (w/v) ice-cold 10 mM phosphate buffer (pH 6.5) containing 0.1% NP-40 using a tissue grinder. After centrifugation at 14 000× *g* for 10 min, the supernatant was retained. After protein quantitation, 100 µg protein was subjected to IL-1β assay by ELISA according to the protocol provided by the manufacturer. The concentration of IL-1β was calculated from a standard curve.

Assesement of stability against microsomal enzymes

Incubation of PTIQ in the presence of microsomal preparations was carried out according to the instructions provided by BD Biosciences. The reaction mixture (1 mL final) consisting of 1 µM PTIQ, the liver microsomal protein (1 mg·mL^{-1}), NADPH-regenerating system without NADPH (10 mM glucose-6-phosphate, 0.2 U·mL^{-1} glucose-6-phosphate dehydrogenase and 9.2 mM $MgCl_2$), and 100 mM potassium phosphate (pH 7.4) was pre-incubated for 5 min at 37°C. The reaction was initiated by addition of NADPH (1.2 mM). At 0, 15, 30, 45 and 60 min, samples (100 µL) were taken from the

reaction, mixed with acetonitrile (1:4 v/v), and centrifuged at 20 000× *g* for 5 min. The supernatant was transferred into a 96-well plate and analysed by LC/MS/MS to determine the amount of remaining PTIQ.

In vitro *assays for CYP inhibition*

Inhibition of CYP was determined from the IC_{50} measured for five CYP isozymes (3A4, 2D6, 2C9, 2C19 and 1A2), according to the instructions provided by the manufacturer. The reaction contained the corresponding buffer, cDNA-overexpressed P450 supersome and fluorescent substrate for each subtype (CYP3A4, 7-benzyloxy-4-triuoromethyl-coumarin; CYP2D6, 3-[2-(N,N-diethyl-N-methyl-amino) ethyl]-7-methoxy-4-methyl-coumarin; CYP2C9, 7-methoxy-4-trifluoro-methyl-coumarin; CYP2C19, 3-cyano-7-ethoxy-coumarin; and CYP1A2, 3-cyano-7-ethoxy-coumarin) and various concentrations of PTIQ in a total volume of 50 µL. The reaction was terminated by the addition of four times the volume of acetonitrile. Fluorescence per well was measured using a fluorescent plate scanner, and each metabolite of the fluorescent substrates was also analysed by LC/MS/MS. The IC_{50} values were determined using Prism v5.0 (GraphPad software, La Jolla, CA, USA).

HEK293 cell culture and whole-cell patch clamp recording

HEK293 cells. stably expressing human ether-à-go-go related gene (hERG) channels (a kind gift from Dr. C. January; Zhou *et al.*, 1998), were cultured in minimum essential medium supplemented with 10% FBS, 1 mM sodium pyruvate, 0.1 mM non-essential amino-acid solution, 100 units·mL^{-1} penicillin G sodium, 100 µg·mL^{-1} streptomycin sulphate and 400 µg·mL^{-1} geneticin. Whole-cell currents were recorded using standard patch clamp techniques. The external solution contained 136 mM NaCl, 5.4 mM KCl, 1.8 mM $CaCl_2$, 1 mM $MgCl_2$, 10 mM glucose and 10 mM HEPES (adjusted to pH 7.4 with NaOH). The intracellular solution contained 130 mM KCl, 1 mM $MgCl_2$, 10 mM EGTA, 5 mM MgATP and 10 mM HEPES (adjusted to pH 7.2 with KOH). The pipette had resistance of 2–4 MΩ. All experiments were performed at 22 ± 1°C. Cells were held at –80 mV and depolarized to +20 mV for 4 s, and then clamped to –50 mV for 6 s before returning to –80 mV. These pulses were repeated every 30 s until the current amplitude reached the steady state in the absence and presence of PTIQ.

Measurement of plasma and brain PTIQ

Male ICR mice (Orient Corp.) were injected i.p. with PTIQ (30 mg kg^{-1}), and anesthetized with diethyl ether by inhalation. At 2 and 5 min, the posterior vena cava was exposed and 0.7 mL blood was drawn with a 23 G needle. The animal was then immediately perfused with 10 mL ice-cold PBS at the flow rate of 2 mL·min^{-1} through the vena cava and the jugular vein. The brain was removed from the skull and washed twice with PBS. The tissue was homogenized in 4-fold (w/v) ice-cold PBS solution at 1500 rpm for 40 s using Kinematica polytron PT2100 homogenizer (Bohemia, NY, USA) and sonicated for 5 min using sonic ultrasonicator microtip (Newtown, CT, USA). Four volumes of acetonitrile containing internal standard were added to the brain homogenate and plasma samples, and the mixture was vortexed vigorously for 5 min. After centrifugation at 20 000× *g* for 10 min, the supernatant was analysed by LC/MS/MS.

Data analyses

Data are expressed as mean ± SEM. Comparisons of three or more groups were analysed by one-way ANOVA and made using the *post hoc* Dunnett's multiple comparison test and Tukey's multiple comparison test. Statistical tests were carried out using Prism. A value of $P < 0.05$ was considered statistically significant for all analyses.

Materials

Culture media, FBS, L-glutamine, trypsin/EDTA, and penicillin-streptomycin were purchased from GibcoBRL (Gaithersburg, MD, USA). LPS, MPTP and PMSF were purchased from Sigma Chemical (St. Louis, MO, USA). The first strand cDNA synthesis kit for reverse transcription PCR (RT-PCR) was obtained from MBI Fermentas (Burlington, ON, Canada), the TNF-α ELISA kit and IL-1β ELISA kit were from eBioscience (San Diego, CA, USA), and Bradford protein assay kit was from Bio-Rad (Hempstead, UK). Primary antibodies used were goat polyclonal antibody to MMP-3 from R&D Systems Inc. (Minneapolis, MN, USA), rabbit polyclonal antibody to NF-κB p65 subunit, goat polyclonal to lamin B and goat polyclonal antibody to COX-2 from Santa Cruz Biotechnology (Santa Cruz, CA, USA), rabbit polyclonal antibody to TH from Protos (New York, NY, USA), mouse monoclonal antibody to TH from Chemicon (Temecula, CA, USA), rabbit polyclonal antibody to β-actin from Enzo Life Sciences (Postfach, Lausen, Switzerland) and rabbit polyclonal antibody against Iba-1 from Wako Chemicals (Osaka, Japan). Human, rat, dog, monkey and mouse liver microsomes and baculovirus/insect cell-expressed human cytochrome P450 (CYP) isozymes were obtained from BD Biosciences (San Jose, CA, USA). Vectastain ABC kit and biotinylated secondary antibodies were purchased from Vector Laboratories (Burlingame, CA, USA) and FluoroJade C was from Histochem Inc. (Jefferson, AR, USA). Chemiluminescence detection system was obtained from Pierce Chemical (Rockford, IL, USA). Chemicals used in organic synthesis were purchased from Aldrich (St. Louis, MO, USA), Acros (Geel, Belgium) or Tokyo Chemical Industry (Tokyo, Japan). Dichloromethane, ethyl acetate and hexane were used after simple distillation. TLC silica gel glass plates (0.25 mm) containing F-254 indicator were obtained from Merck (Rahway, NJ, USA). All other chemicals were reagent grade and were purchased from Sigma Chemical or Merck.

Results

PTIQ suppresses MMP-3 induction in stressed dopaminergic cells and provides protection

We have previously established that exposure to tetrahydrobiopterin (BH4), a compound normally present in dopaminergic cells, causes oxidative stress (Choi *et al.*, 2000; 2003; Lee *et al.*, 2007a) and up-regulation of MMP-3 (Choi *et al.*, 2008) in cultured dopaminergic CATH.a cells as well as primary cultured mesencephalic dopaminergic neurons. Using this

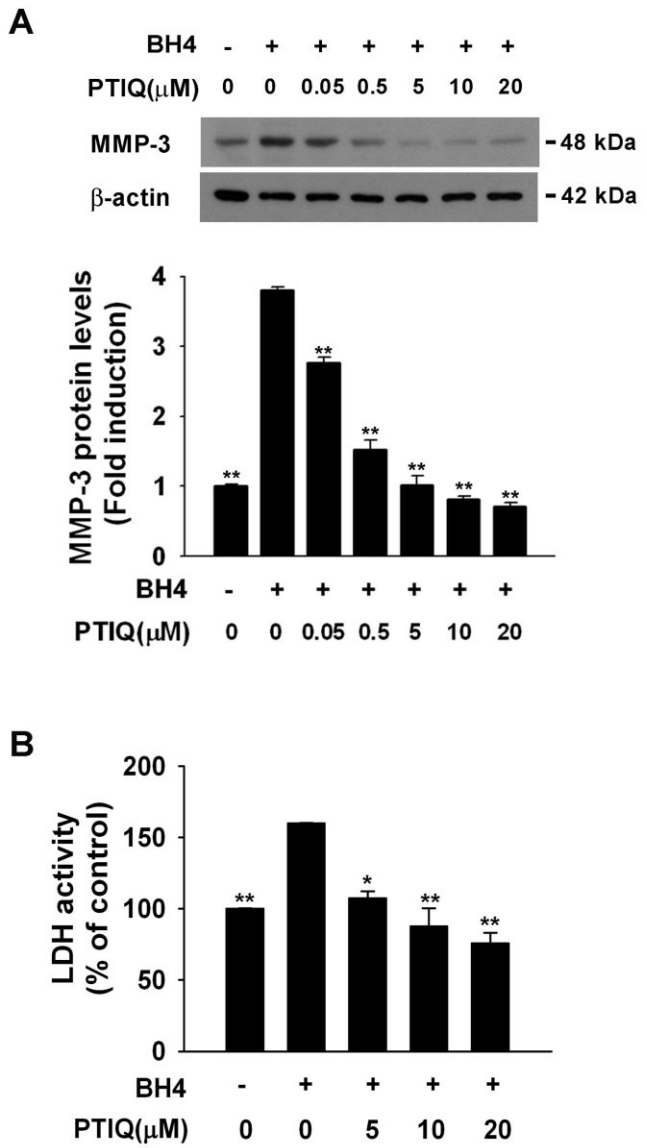

Figure 2

PTIQ suppresses cell stress-induced MMP-3 production in dopaminergic cells and provides protection. CATH.a cells were exposed to 100 μM BH4 in the presence of various concentrations of PTIQ. (A) The cells were harvested after 24 h and the level of intracellular MMP-3 was assessed by Western blot analysis. The data are expressed as fold induction of untreated control (mean ± SEM). (B) CATH.a cells were exposed to BH4 for 24 h, and cell death were assessed by LDH activity in the culture medium. The data are expressed as % of untreated control ± SEM; *$P < 0.05$; **$P < 0.01$, significantly different from BH4-treated.

system, we first tested whether PTIQ might suppress the induction of MMP-3. As shown in Figure 2A, the dramatic up-regulation of MMP-3 (3.8-fold of untreated control) induced by BH4 was suppressed by co-treatment with PTIQ. A statistically significant suppression was achieved at 50 nM (60% of BH4-alone control) and complete suppression was obtained at around 5 μM. The IC_{50} of PTIQ for MMP-3 induction was calculated to be 60 nM.

Because MMP-3 contributed to cell death and PTIQ suppressed induction of MMP-3, it was possible that PTIQ might provide cytoprotection. Consistent with our previous data, CATH.a cells treated with BH4 showed an increase in cell death (160% of untreated control; Figure 2B), determined by activity of LDH released into the medium. Co-treatment with 5 μM PTIQ gave complete protection of the cells and the IC_{50} value for the protection was calculated to be 1.8 μM.

PTIQ suppresses the MMP-3 induction and proinflammatory responses in activated microglia

The effect of PTIQ on MMP-3 in activated microglia was tested. The murine microglial cell line BV-2 was challenged with LPS (0.2 μg mL^{-1}) in the presence or absence of various concentrations of PTIQ, and changes in MMP-3 mRNA level were determined by RT-PCR (Figure 3A). PTIQ suppressed the mRNA for MMP-3 completely at 5 μM, to 13% of LPS-alone control, accompanied by decreased MMP-3 protein, as determined by Western blot analysis (Figure 3B). The IC_{50} of PTIQ for inhibiting MMP-3 protein production was calculated to be 2.4 μM.

Because MMP-3 has been reported to be correlated with the expression of IL-1β and TNF-α (Mun-Bryce *et al.*, 2002; Nuttall *et al.*, 2007; Woo *et al.*, 2008), the cytotoxic cytokines known to exert damaging effects on dopaminergic neurones (Carvey *et al.*, 2005), it was possible that these cytokines might also be down-regulated after PTIQ exposure. Results of RT-PCR revealed that the mRNA levels of IL-1β and TNF-α (Figures 3C and 3D), which were dramatically increased by LPS, were dose-dependently reduced in the presence of PTIQ. A concentration as low as 2.5 μM had a statistically significant lowering effect, 100 μM PTIQ caused reduction of IL-1β and TNF-α to 10% and 36% of LPS-alone control, respectively. The protein level of TNF-α increased by LPS was also attenuated by PTIQ in a dose-dependent manner (Figure 3E), and the IC_{50} was calculated to be 6.5 μM. COX-2, another enzyme involved in inflammatory responses (Bazan, 2001), was also down-regulated by PTIQ in a dose-dependent manner. The COX-2 mRNA level increased by LPS was reduced to 38% of LPS-alone control by 2.5 μM PTIQ and further reduction was achieved at higher concentrations (Figure 3F). The COX-2 protein level was similarly suppressed by PTIQ (Figure 3G), with an IC_{50} value of 9.3 μM.

As the mechanism by which MMP-3 is induced in activated microglia is thought to involve the nuclear translocation of the transcription factor NF-κB (Borghaei *et al.*, 2009), we tested whether PTIQ might affect the NF-κB system. Western blot analysis (Figure 3H) showed a dramatic increase in the NF-κB p65 subunit in the nuclear fraction of BV-2 cells that had been challenged with LPS. On the other hand, co-treatment with PTIQ completely abolished this effect.

PTIQ alleviates motor deficits in an animal model of Parkinson's disease

Whether PTIQ might provide neuroprotective effects *in vivo* was determined in an animal model of Parkinson's disease generated by administration of the dopaminergic toxin MPTP. Two PTIQ doses were tested (3 or 30 mg kg^{-1}, i.p.) and the animals were first subjected to various behavioural tests for evaluation of their motor activity. On hindlimb test

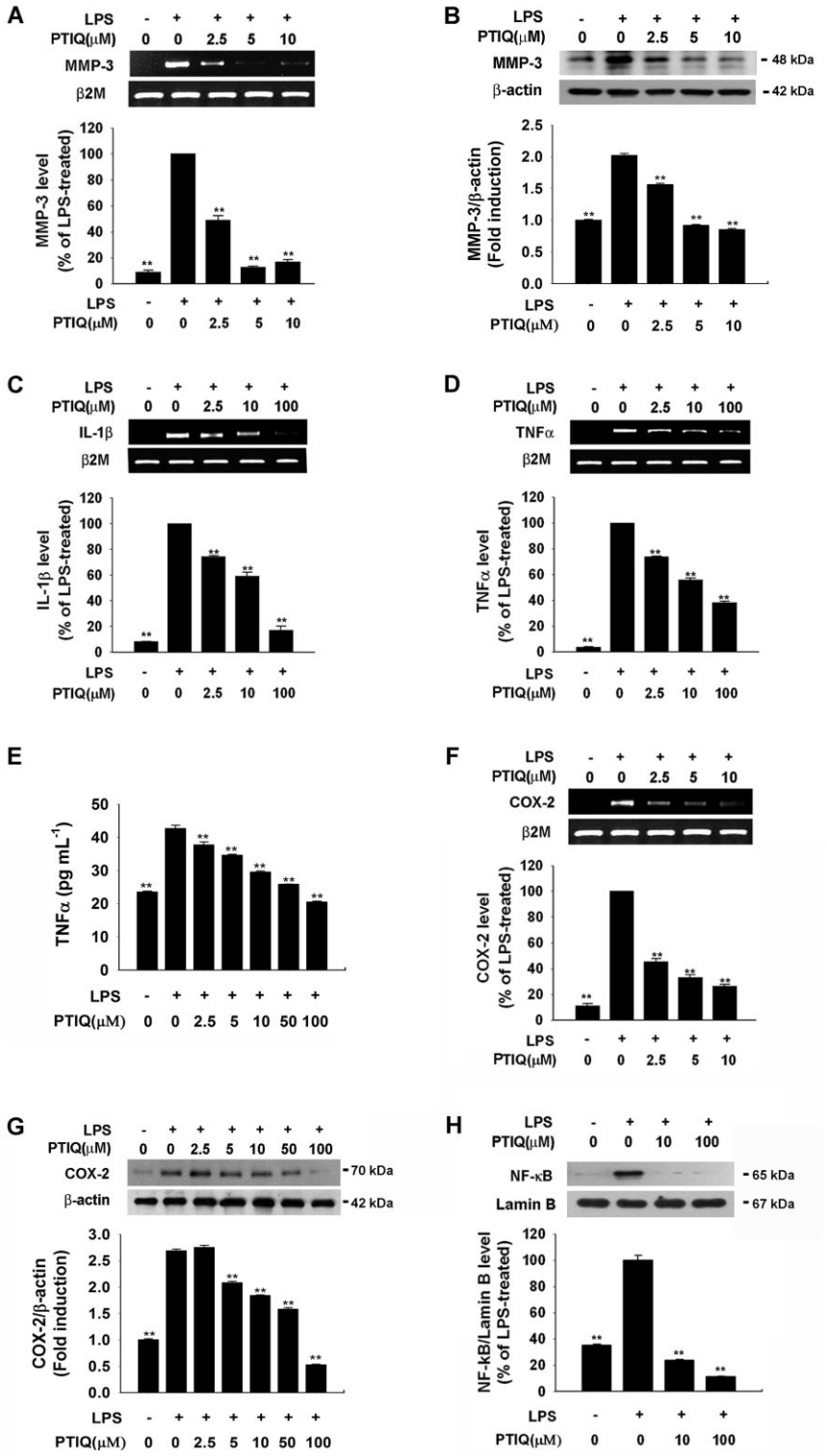

Figure 3

PTIQ suppresses gene expression of MMP-3, IL-1β, TNF-α and COX-2 and nuclear translocation of NF-κB p65 in activated microglia. BV-2 cells were treated with LPS (0.2 μg mL^{-1}) alone or with various concentrations of PTIQ. After 6 h, total RNA was isolated and subjected to RT-PCR for (A) MMP-3 (C) IL-1β (D) TNF-α, and (F) COX-2, each with β2 microglobulin (β2M) as an internal standard. After 24 h, cell lysate was subjected to Western blot analysis for(B) MMP-3 and (G) COX-2, each with β-actin as loading control, and to ELISA for TNF-α (E). After 1 h, nuclear proteins were obtained, 5 μg of which was subjected to Western blot analysis against NF-κB p65 and lamin B (loading control) (H). The results are mean ± SEM of three independent experiments. $^{**}P < 0.01$, significantly different from LPS-treated. Top panels, typical agarose gel electrophoresis of RT-PCR products or Western blot; Bottom panels, densitometric quantitation normalized against respective loading controls.

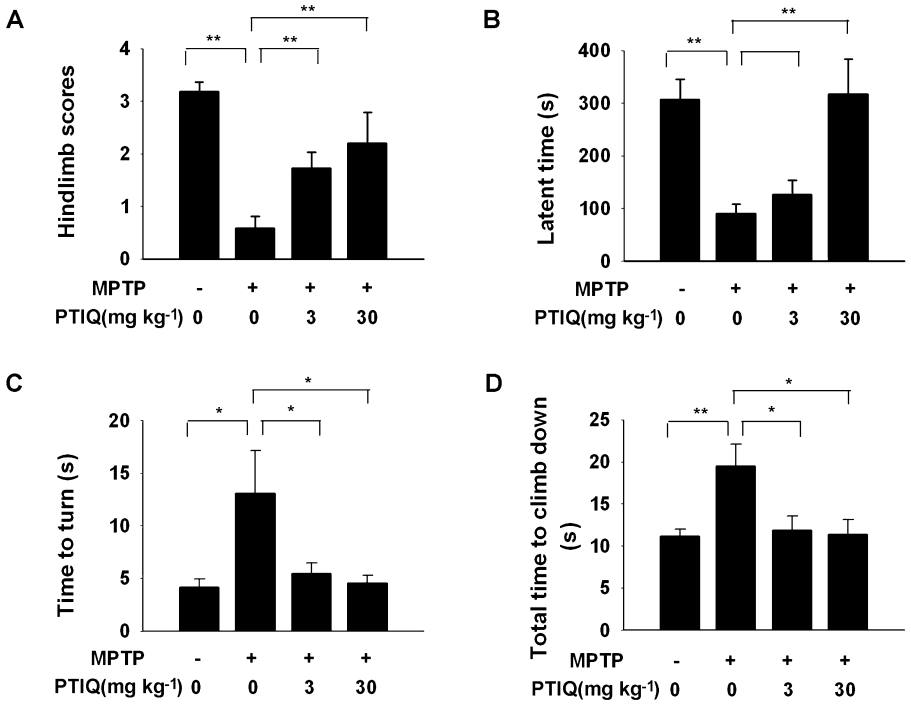

Figure 4

PTIQ alleviates motor deficits in MPTP-induced Parkinson's disease mice. Motor deficits of animals treated with MPTP alone or cotreated with PTIQ were assessed by the hindlimb test (A), rotarod test (B), and vertical grid test (C, D). The results are shown as means ± SEM. *$P < 0.05$; **$P < 0.01$, significantly different as shown.

(Figure 4A), the MPTP-treated animals in general showed weakness of postural balance, consistent with the previously published results (Muralikrishnan and Mohanakumar, 1998). In comparison, the animals treated with 3 and 30 mg·kg^{-1} of PTIQ exhibited considerable improvement. On the rotarod test (Figure 4B), the time spent on the rotarod decreased in the MPTP-treated animals, but was similar to control values in the animals that had been treated with 30 mg kg^{-1} of PTIQ. The animals treated with 3 mg kg^{-1} of PTIQ appeared to show improved motor activity but this effect was not statistically significant. On the vertical grid test, another behavioural test demonstrated to provide a reliable measure of Parkinson's disease-related motor activity (Kim *et al.*, 2010b), the MPTP mice took much longer to turn around and to climb down on the vertical grid box, compared with the vehicle-treated control (Figure 4C and 4D). The animals treated with PTIQ at both 3 and 30 mg·kg^{-1} significantly improved the score on vertical grid, as they took shorter time to turn and to climb down. Taken together, treatment with either 3 or 30 mg·kg^{-1} PTIQ attenuated the motor deficits specific to Parkinson's disease animal models, with 30 mg·kg^{-1} generally having a greater effect.

PTIQ protects the nigral dopaminergic neurones and striatal dopaminergic terminals in the animal model of Parkinson's disease

We tested whether the improvement of motor activities in the PTIQ-treated animals might be accompanied by survival of the nigral dopaminergic neurons. The MPTP treatment led to a clear loss of the TH-immunopositive dopaminergic neurones in the SN (Figure 5A). In the MPTP animals cotreated with PTIQ, the number of dopaminergic neurones remained at control levels ($P > 0.05$). PTIQ alone had no effect on TH-immunoreactive cells. FluoroJade C staining, which detects degenerating cells, revealed that the number of FluoroJade C-positive cells in the nigral region was increased by the MPTP treatment, but not in the animals treated with PTIQ (Figure 5B).

The effects of PTIQ on the dopaminergic terminals in the striatum, the brain region to which the nigral dopaminergic neurones project their fibres and where dopaminergic neurodegeneration first occurs in Parkinson's disease, was also tested. A marked decrease in the density of TH-immunoreactive fibres was noted in the striatum of the MPTP-treated animals, but this was prevented in the animals given PTIQ (Figure 5C). This decrease was also evident in Western blots for TH in the striatal tissue of these animals (Figure 5D). TH protein level was decreased in the MPTP-treated animals but was unchanged in the MPTP–PTIQ-treated animals ($P > 0.05$). In agreement with the *in vitro* results, this *in vivo* neuroprotection by PTIQ was accompanied by suppression of MMP-3 protein (Figure 5E).

PTIQ lowers neuroinflammation in the SN in the animal model of Parkinson's disease induced by MPTP

The nigral sections were also analysed by immunostaining for Iba-1, a microglial marker protein (Sierra *et al.*, 2007)

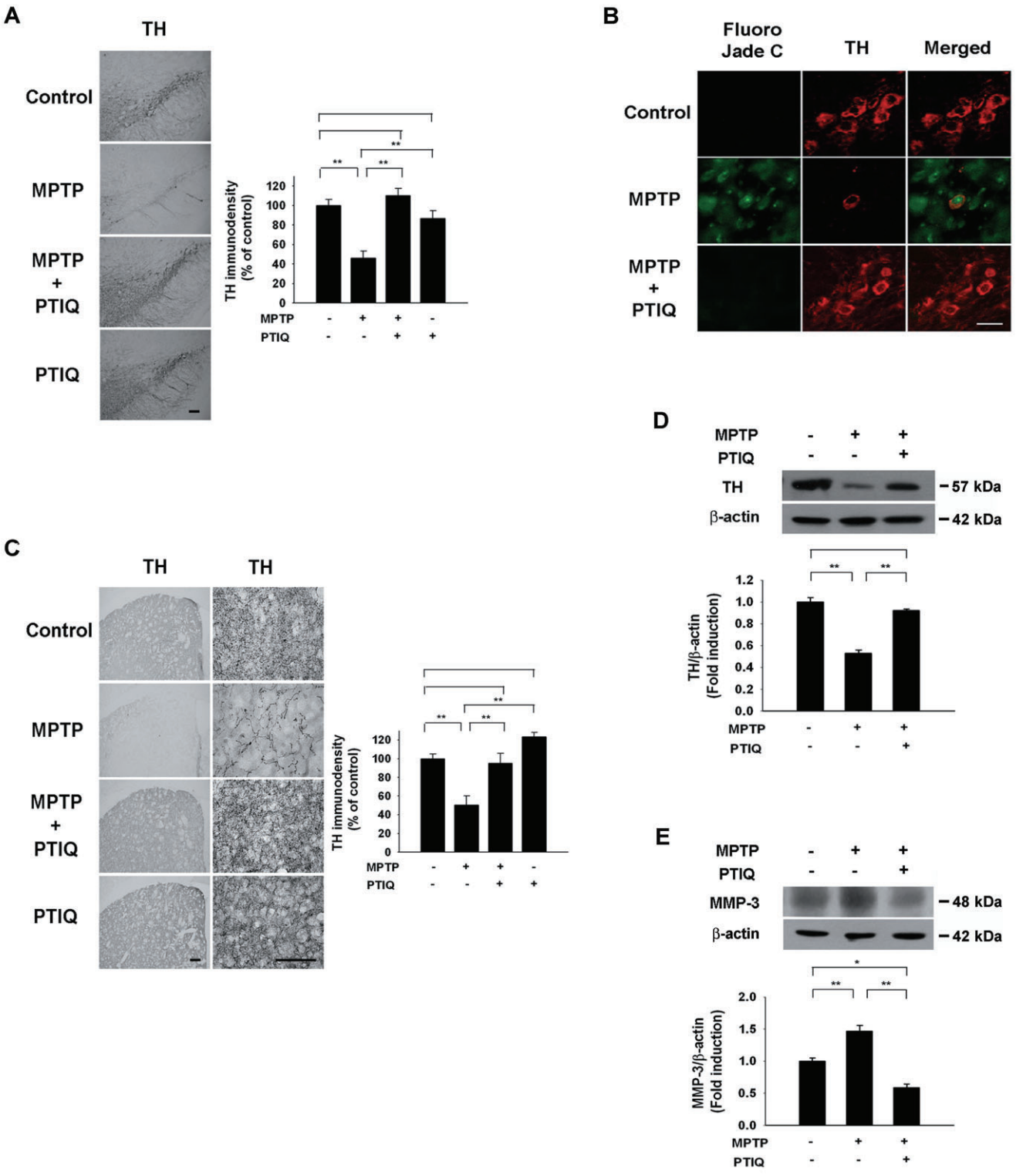

Figure 5

PTIQ protects the nigrostriatal system against MPTP-elicited neurodegeneration. (A) SN sections of mice treated with MPTP alone or with PTIQ were examined for immunoreactive TH and developed in diaminobenzidine to detect dopaminergic neurons. (B) The sections were also double-fluorostained with FluoroJade C and TH to show degeneration. (C) Striatal sections were immunostained for TH and developed in diaminobenzidine to detect dopaminergic fibers. Quantitative analysis of TH-immunopositive neurones was performed and the data are expressed as percent of vehicle-treated control (mean ± SEM). Striatal tissue homogenate was subjected to Western blot analysis for (D) TH and (E) MMP-3, each with β-actin as normalizing control. Quantitation was made by densitometry and the data are expressed as fold induction of vehicle-treated control ± SEM. Scale bars = 20 μm (B) and 100 μm (A, C). *$P < 0.05$; **$P < 0.01$, significantly different as shown.

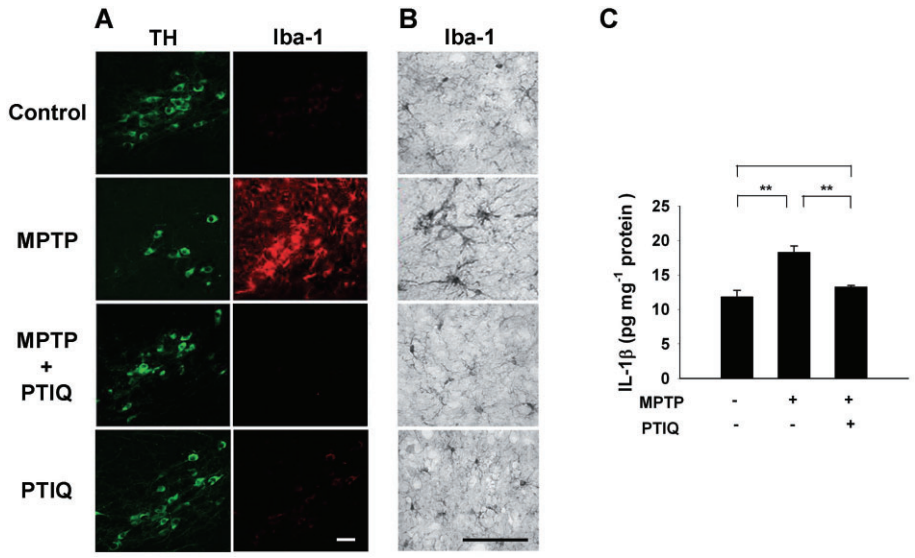

Figure 6

PTIQ prevents microglial activation in the SN of MPTP-induced mice. SN sections of mice treated with MPTP alone or with PTIQ were double immunofluorostained for TH to identify dopaminergic neurones and Iba-1 to identify microglial cells (A). The sections were also immunostained for Iba-1 and developed in diaminobenzidine (B). SN tissue homogenate was subjected to ELISA against IL-1β (C). Scale bars = 40 μm. $^{**}P < 0.01$, significantly different as shown.

(Figure 6A and 6B). Upon MPTP administration, the ramified morphology of resting microglia in the saline-treated mice became ameboid, indicative of activation, and they were localized in close proximity to the damaged dopaminergic neurones in the nigra. In the animals cotreated with PTIQ and MPTP, the Iba-1 immunoreactive cells were not morphologically different from those of the vehicle-treated control. PTIQ alone had no apparent effect on Iba-1 immunoreactive cells. The MPTP treatment also caused an increase in IL-1β protein level to 155% in the nigral area, but this was suppressed by PTIQ ($P > 0.05$ vs. vehicle-treated control).

PTIQ is resistant to metabolism by liver microsomal enzymes

For a compound to be utilized as a drug, a number of pharmacokinetic requirements must be met. In order to assess bioavailability of PTIQ, the degree of its modification by the liver microsomal enzymes from various species was determined *in vitro* (Figure 7). PTIQ was found to be quite resistant to human, rat, dog, monkey and mouse drug metabolizing enzymes, as shown by the proportion of PTIQ remaining after a 60 min incubation with microsomal enzyme preparations. The compound was most stable against female human microsomal preparation and least stable against the female mouse microsomal preparation. PTIQ appeared more stable against female than male in human and rat microsomes and male than female in monkey, dog, and mouse. The metabolic stability of PTIQ was comparable with suberoylanilide hydroxamic acid (SAHA, vorinostat), a compound known to be metabolically stable (Venkatesh *et al.*, 2007).

The IC_{50} values of PTIQ against CYP isoforms are high

To assess the possibility of drug–drug interactions, we tested the effect of PTIQ on enzyme activities of CYP subtypes: 1A2, 2D6, 2C9, 2C19 and 3A4. As shown in Table 1, the IC_{50} of PTIQ for the subtypes ranged from 112 μM to 760 μM, as determined by the fluorescence detection method (Bell *et al.*, 2008). The results were confirmed by another analytical method using LC/MS/MS: the IC_{50} of PTIQ for the CYP subtypes ranged from 97 μM to >810 μM.

PTIQ has a good safety profile

To assess possible cytotoxic effect of PTIQ *in vivo*, hepatocyte morphology was evaluated after administration of PTIQ (two i.p. injections at 30 mg kg^{-1}, 24 h apart). There were no apparent morphological differences in the hepatocytes of the PTIQ- and saline-treated mice (Figure 8A). We also performed a single-dose acute toxicity test. When administered at various doses, the mice survived up to 1000 mg·kg^{-1} PTIQ, given i.p.. Autopsy of these animals revealed no apparent organ damage. Higher doses were not tested due to shortage of PTIQ available to us.

We also tested for a possible side effect of PTIQ on the human ERG potassium channel, as interference with this channel activity has been correlated with serious cardiac arrhythmias (Recanatini *et al.*, 2005). Patch clamp analysis of hERG channel activity expressed in HEK293 cells showed that the current did not change in the presence of PTIQ at a concentration as high as 500 μM (Figure 8B).

PTIQ readily enters the brain

For PTIQ to be utilized as a neuroprotective agent, its entry to the brain would be a prerequisite. To test this possibility, mice

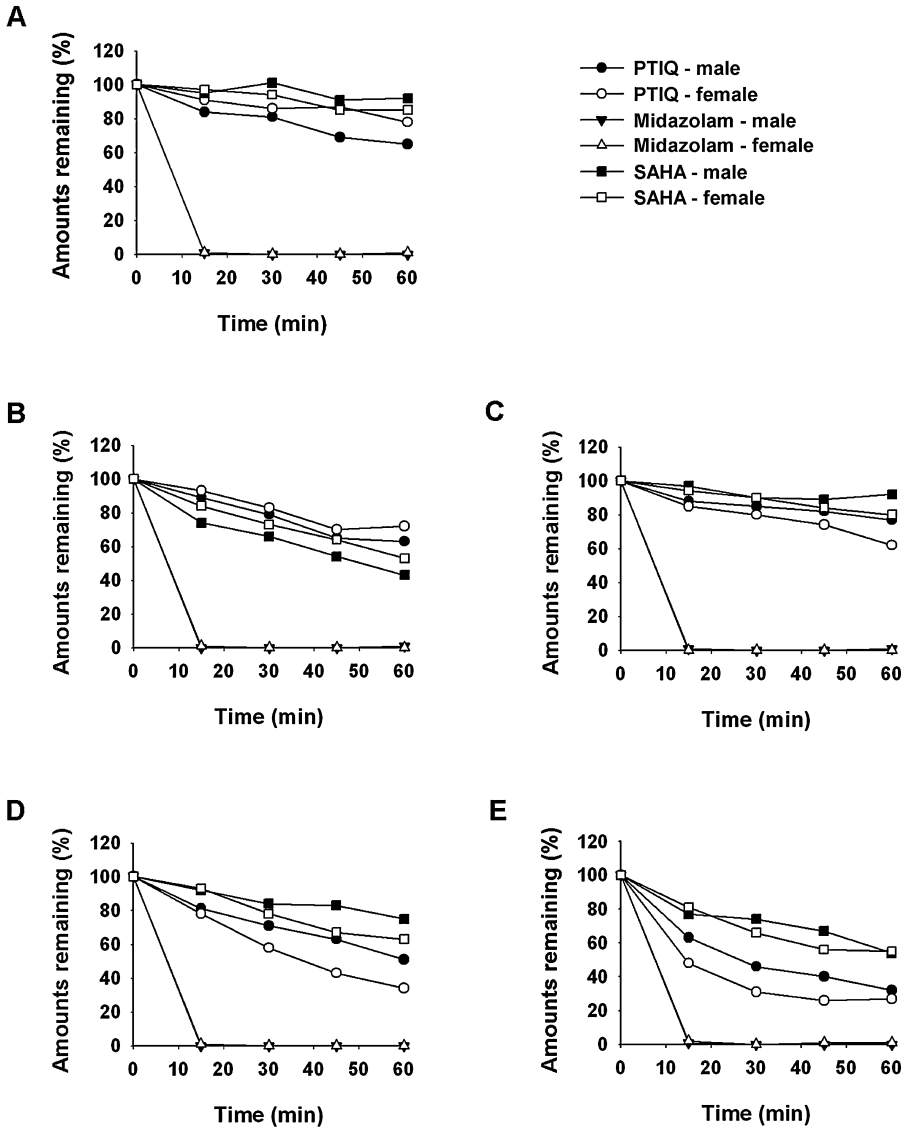

Figure 7

PTIQ is stable against liver microsomal enzymes. PTIQ was incubated with liver microsomal preparations from human (A), rat (B), dog (C), monkey (D), and mouse (E) in the presence of NADPH-regenerating system for various time periods. The amount of remaining PTIQ was assessed by GC-HPLC. Results shown are means + SEM of three independent experiments. SAHA, suberoylanilide hydroxamic acid.

were given PTIQ (30 mg kg^{-1}, i.p.) and its levels in the plasma and brain were determined. At 5 min after i.p. injection of PTIQ, the concentrations of PTIQ in the brain and plasma were 2.59 ng mL^{-1} and 9.30 ng mL^{-1}, respectively, with the brain:plasma ratio calculated to be 0.28 (Table 2).

Discussion

In the present study we demonstrate that our synthetic compound PTIQ provided protection of the nigral dopaminergic neurones in the mouse model of Parkinson's disease elicited by MPTP and improved the associated motor deficits. The compound exerted both protection of the dopaminergic cells via suppression of MMP-3 production and inhibition of inflammatory mechanisms involving down-regulation of expression of MMP-3 as well as IL-1β, TNF-α and COX-2 in activated microglial cells. PTIQ entered the brain, was stable against liver microsomal enzymes, and did not inhibit hERG channels or CYP isozyme activities, making it a good candidate compound as a drug for the CNS.

The current treatment for Parkinson's disease is mainly focused on alleviation of the symptoms using the dopamine precursor L-DOPA. Unfortunately, chronic treatment with L-DOPA often causes motor and psychiatric side effects (Fahn, 1989) and evidence suggests that L-DOPA itself may be neurotoxic at least in animals (Emdadul *et al.*, 2003). None of the currently available therapies, however, can delay the degeneration itself.

Table 1

IC_{50} values of PTIQ for various CYP isoforms

CYP isoforms	IC_{50} (μM) by the fluorescence method		IC_{50} (μM) by the LC/MS/MS method		
	PTIQ	Reference inhibitor	PTIQ	Reference inhibitor	Reference inhibitor used
3A4	533	0.8	468	0.2	Ketoconazole
2D6	760	0.0	>810	0.0	Quinidine
1A2	220	1.0	168	1.0	Furafylline
2C9	112	0.2	168	1.0	Sulfaphenazole
2C19	119	3.0	97	0.3	Tranylcypromine

Specific enzyme activity was estimated for each CYP isoforms, using the respective reference inhibitor, substrate, cDNA-expressed CYP enzyme and various concentrations of PTIQ as described in Methods. The IC_{50} value was determined for each enzyme using Prism, v5.0 (GraphPad software).

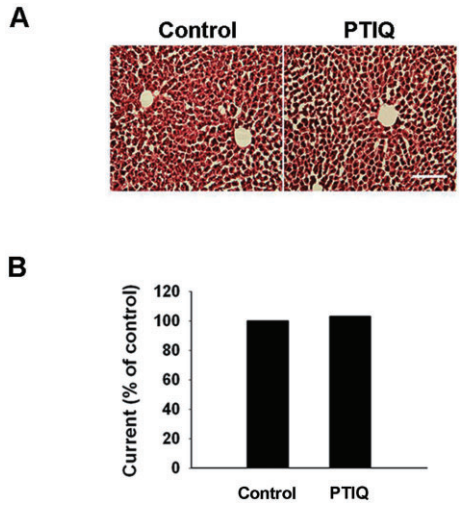

Figure 8

PTIQ has no adverse effect on hepatocyte morphology or hERG channel activity. (A) Liver sections of mice treated with 30 mg kg^{-1} PTIQ were stained with hematoxylin and eosin. Scale bar = 100 μm. (B) Effect of PTIQ in hERG channel was tested at a concentration of 500 μM by the whole-cell patch clamp recording method and expressed as the current in percent of untreated control.

Table 2

Amounts of PTIQ in the plasma and brain after i.p.injection

Time (min)	Concentration (ng mL^{-1}) Brain	Plasma	B/P ratio
2	2795	10 354	0.27
5	2586	9 303	0.28

Male ICR mice were given PTIQ (30 mg kg^{-1} i.p.) and the brain was extracted and blood collected at 2 and 5 min. The blood and brain samples were processed and analysed by LC/MS/MS for PTIQ measurement.

Because the clinical symptoms of Parkinson's disease are not manifest until more than 70% of the nigral dopamine neurones have degenerated, ways to halt or delay the degenerative progression in the presymptomatic, early stage of degeneration would be highly beneficial. Early detection of Parkinson's disease is now available with the advances in brain imaging techniques such as PET and functional MRI (fMRI). Toward this goal, we have recently developed a method to produce [^{18}F]fluoropropylcarbomethoxyiodophenylnortropane ([^{18}F]FP-CIT), a high affinity dopamine transporter ligand, at a high radiochemical yield and reproducibility to be utilized for high resolution imaging for early diagnosis of Parkinson's disease by PET (Lee *et al.*, 2007b). Once the presymptomatic Parkinson's disease patients have been identified, disease-modifying, neuroprotective therapy that delays the neurodegenerative process can greatly improve the quality of life of these individuals. Towards such a goal, we have previously reported syntheses and effects of new compounds (Seo *et al.*, 2005; 2008).

Interfering with apoptotic signalling has been a key issue in the development of disease-modifying therapy. Caspase inhibitors are unsuitable because of the large quantities required and lack of passage through the blood–brain barrier (BBB) (Charriaut-Marlangue, 2004). Another potential cellular target is MMP-3 because it is increased only under cell stress conditions and in turn, participates in apoptotic signalling (Choi *et al.*, 2008; Kim *et al.*, 2010a). Indeed, down-regulation of MMP-3 by various approaches leads to cytoprotection *in vitro* (Choi *et al.*, 2008; Kim *et al.*, 2010a), and MMP-3 knockout mice show resistance to MPTP-elicited nigral neurodegeneration (Kim *et al.*, 2007). While numerous MMP-3 inhibitors have been developed, it is likely that the relatively large peptide-based inhibitors of MMP-3 will not efficiently cross the BBB. Most non-peptidic MMP inhibitors that have been reported thus far contain hydroxamic acid, carboxylic acids, phosphonates or thiols and, as such, may not easily enter the brain. Poor solubility of the most commonly used MMP inhibitors is another disadvantage. In addition, administration of MMP-3-specific siRNA would require a

rather invasive, direct injection into the brain. We have here demonstrated that our compound PTIQ can suppress MMP-3 production, can enter the brain and provide neuroprotection.

Increasing experimental evidence has shown that inhibition of the neuroinflammatory reaction can attenuate degeneration of dopaminergic neurones in several models of Parkinson's disease (Wu *et al.*, 2002; Hirsch and Hunot, 2009). Because of this, neuroprotective therapies have been designed against neuroinflammation. The steroid dexamethasone has been reported to attenuate the degeneration of dopamine-containing neurones induced by MPTP (Kurkowska-Jastrzebska *et al.*, 1999) or LPS (Castaño *et al.*, 2002). However, steroids have limitations for long-term use in clinical situations due to side effects. Although non-steroidal anti-inflammatory drugs, such as salicylic acid, are able to attenuate MPP^+-induced striatal dopamine depletion (Sairam *et al.*, 2003), there is no clinical evidence supporting their neuroprotective effect. In addition, the tetracycline derivatives minocycline (Du *et al.*, 2001; Tikka *et al.*, 2001; Wu *et al.*, 2002) and doxycycline (Cho *et al.*, 2009) have shown to inhibit neuroinflammation both *in vitro* and in animal models, but requirements for a high dose are of concern if the drugs were to be administered to patients (Thomas *et al.*, 2003). In fact, during the ongoing clinical trial for Parkinson's disease, the issue of decreased tolerability of minocycline has recently been raised (NINDS NET-PD Investigators, 2008). We show in the current study that PTIQ, which is not a steroid and not an antibiotic, may be a useful anti-inflammatory neuroprotectant, as it suppressed the induction of MMP-3, the cytotoxic cytokines and COX-2 *in vitro*, and attenuated microglial activation and protected the nigral dopaminergic neurones *in vivo*.

A structurally related compound, 1-methyl-1,2,3,4-tetrahydroisoquinoline (1-methyl-TIQ), is present in the brain and exhibits neuroprotective effects both *in vitro* and *in vivo* (Tasaki *et al.*, 1991; Abe *et al.*, 2005; Kotake *et al.*, 2005; Antkiewicz-Michaluk *et al.*, 2006). Further, some derivatives of 1-methyl-TIQ exert even a higher neuroprotective effect (Okuda *et al.*, 2006; Katagiri *et al.*, 2010). The effect of TIQ derivatives on microglial system had not been reported thus far to our knowledge. TIQ derivatives have been reported to cross the BBB (Abe *et al.*, 2005), supporting our results that PTIQ readily enters the brain. On the other hand, some TIQ derivatives, such as *N*-methyl-1,2,3,4-tetrahydroisoquinoline (*N*-methyl-TIQ), 1-benzyl-1,2,3,4-tetrahydroisoquinoline (1-benzyl-TIQ) and 6,7-dihydroxy-1-methyl-1,2,3,4-tetrahydroisoquinoline (salsolinol), are thought to be cytotoxic (Nagatsu, 1997; Antkiewicz-Michaluk *et al.*, 2000; Lorenc-koci *et al.*, 2000). These toxic TIQs are distinct in chemical structure from PTIQ in that they have a catechol residue, which can be readily oxidized (Schweigert *et al.*, 2001) or have an imine group that can form a reactive polyaromatic ring (Tang *et al.*, 2003).

PTIQ was shown to possess a good pharmacokinetic profile as a candidate drug. Firstly, it entered the brain. Obviously, penetration of the BBB is an important factor in development of a drug targeted to the brain, and many compounds that show neuroprotective effect *in vitro* have been dismissed due to low penetration of the BBB (Pardridge, 2005). Secondly, PTIQ shows a good metabolic stability. In drug discovery, especially when using a high-throughput-based pharmacological process, metabolic stability evaluated *in vitro* is an important criterion in determining whether to continue further development (Rodrigues, 1997). The findings that a majority of PTIQ was unchanged after incubation with liver microsomal enzymes and that highest stability was obtained against the human enzymes among the various species tested, suggest that the compound may have high bioavailability when administered in humans. Our finding that PTIQ was the least stable against mouse microsomal enzymes and yet provided protection in mice is quite promising in this regard. Thirdly, PTIQ is not likely to cause side effects derived from drug–drug interaction. Metabolism-related drug–drug interactions *in vivo* can cause adverse reactions or toxic side effects, and this is estimated by *in vitro* screening for drugs that inhibit CYP isozymes, particularly the subtypes 3A4, 2D6, 1A2, 2C9 and 2C19 (Wienkers and Heath, 2005). We have observed that PTIQ has very high IC_{50} values for all of the five isoforms. Fourthly, PTIQ showed no apparent inhibitory effect on the hERG channel. Because a number of compounds have shown to interfere with this channel, leading to a serious cardiac arrhythmia (torsade de pointes) and sudden death (Recanatini *et al.*, 2005), *in vitro* assessment of a drug's effect on the hERG channels has become an important process for safety evaluation at an early stage of drug development (Hancox *et al.*, 2008; Staudacher *et al.*, 2010). We have observed no such adverse effect on the channel, at concentrations as high as 500 μM. Finally, PTIQ showed no apparent acute toxicity when administered *in vivo*. We have observed that 100% of mice administered with 1000 mg kg^{-1} survived with no morphological changes in the organs. Injection of PTIQ i.v. during the pharmacokinetic study at concentrations of 20 mg kg^{-1} did not result in any changes in the animals' behaviour.

In conclusion, we report a novel compound PTIQ, which has anti-inflammatory effects on microglial cells and may be a promising candidate for neuroprotection of the dopaminergic nigral neurones in in the MPTP model of PD.

Acknowledgements

This work was supported by Brain Research Center of the 21st Century Frontier Research Program of the Ministry of Education, Science & Technology (2009 K001252, 2010 K000810 & 2011 K000269) and partly by the National Agenda Project from Korea Research Council of Fundamental Science and Technology, Republic of Korea, to O. Hwang.

Conflict of interest

The authors have no conflict of interest.

References

Abe K, Saitoh T, Horiguchi Y, Utsunomiya I, Taguchi K (2005). Synthesis and neurotoxicity of tetrahydroisoquinoline derivatives for studying Parkinson's disease. Biol Pharm Bull 28: 1355–1362.

Antkiewicz-Michaluk L, Romañska I, Papla I, Michaluk J, Bakalarz M, Vetulani J *et al*. (2000). Neurochemical changes induced by acute and chronic administration of 1,2,3,4-tetrahydroisoquinoline and salsolinol in dopaminergic structures of rat brain. Neuroscience 96: 59–64.

Antkiewicz-Michaluk L, Lazarewicz JW, Patsenka A, Kajta M, Zieminska E, Salinska E *et al*. (2006). The mechanism of 1,2,3,4-tetrahydroisoquinolines neuroprotection: the importance of free radicals scavenging properties and inhibition of glutamate-induced excitotoxicity. J Neurochem 97: 846–856.

Bazan NG (2001). COX-2 as a multifunctional neuronal modulator. Nat Med 7: 414–415.

Bell L, Bickford S, Nguyen PH, Wang J, He T, Zhang B *et al*. (2008). Evaluation of fluorescence- and mass spectrometry-based CYP inhibition assays for use in drug discovery. J Biomol Screen 13: 343–353.

Blasi E, Barluzzi R, Bocchini V, Mazzolla R, Bistoni F (1990). Immortalization of murine microglial cells by a v-raf/v-myc carrying retrovirus. J Neuroimmunol 27: 229–237.

Borghaei RC, Gorski G, Javadi M, Chambers M (2009). NF-kappaB and ZBP-89 regulate MMP-3 expression via a polymorphic site in the promoter. Biochem Biophys Res Commun 382: 269–273.

Carvey PM, Chen EY, Lipton JW, Tong CW, Chang QA, Ling ZD (2005). Intra-parenchymal injection of tumor necrosis factor-alpha and interleukin 1-beta produces dopamine neuron loss in the rat. J Neural Transm 112: 601–612.

Castaño A, Herrera AJ, Cano J, Machado A (2002). The degenerative effect of a single intranigral injection of LPS on the dopaminergic system is prevented by dexamethasone, and not mimicked by rh-TNF-alpha, IL-1beta and IFN-gamma. J Neurochem 81: 150–157.

Charriaut-Marlangue C (2004). Apoptosis: a target for neuroprotection. Therapie 59: 185–190.

Cho Y, Son HJ, Kim EM, Choi JH, Kim ST, Ji IJ *et al*. (2009). Doxycycline is neuroprotective against nigral dopaminergic degeneration by a dual mechanism involving MMP-3. Neurotox Res 16: 361–371.

Choi DH, Kim EM, Son HJ, Joh TH, Kim YS, Kim D *et al*. (2008). A novel intracellular role of matrix metalloproteinase-3 during apoptosis of dopaminergic cells. J Neurochem 106: 405–415.

Choi HJ, Jang YJ, Kim HJ, Hwang O (2000). Tetrahydrobiopterin is released from and causes preferential death of catecholaminergic cells by oxidative stress. Mol Pharmacol 58: 633–640.

Choi HJ, Kim SW, Lee SY, Hwang O (2003). Dopamine-dependent cytotoxicity of tetrahydrobiopterin: a possible mechanism for selective neurodegeneration in Parkinson's disease. J Neurochem 86: 143–152.

Du Y, Ma Z, Lin S, Dodel RC, Gao F, Bales KR *et al*. (2001). Minocycline prevents nigrostriatal dopaminergic neurodegeneration in the MPTP model of Parkinson's disease. Proc Natl Acad Sci U S A 98: 14669–14674.

Emdadul HM, Asanuma M, Higashi Y, Miyazaki I, Tanaka K, Ogawa N (2003). Apoptosis-inducing neurotoxicity of dopamine and its metabolites via reactive quinone generation in neuroblastoma cells. Biochim Biophys Acta 1619: 39–52.

Fahn S (1989). Adverse effects of levodopa in Parkinson's disease. In: Calne DB (ed.). Handbook of Experimental Pharmacology., Vol. 8. Springer: Berlin, Heidelberg; New York, pp. 386–409.

Gantois I, Fang K, Jiang L, Babovic D, Lawrence AJ, Ferreri V *et al*. (2007). Ablation of D1 dopamine receptor-expressing cells generates mice with seizures, dystonia, hyperactivity, and impaired oral behavior. Proc Natl Acad Sci U S A 104: 4182–4187.

Gao HM, Liu B, Zhang W, Hong JS (2003). Novel anti-inflammatory therapy for Parkinson's disease. Trends Pharmacol Sci 24: 395–401.

Hald A, Lotharius J (2005). Oxidative stress and inflammation in Parkinson's disease: is there a casual link? Exp Neurol 193: 279–290.

Hancox JC, McPate MJ, El Harchi A, Zhang YH (2008). The hERG potassium channel and hERG screening for drug-induced torsades de pointes. Pharmacol Ther 119: 118–132.

Hirsch EC, Hunot S (2009). Neuroinflammation in Parkinson's disease: a target for neuroprotection? Lancet Neurol 8: 382–397.

Hurelbrink CB, Armstrong RJ, Luheshi LM, Dunnett SB, Rosser AE, Barker RA (2001). Death of dopaminergic neurons in vitro and in nigral grafts: reevaluating the role of caspase activation. Exp Neurol 171: 46–58.

Hwang O, Baker H, Gross S, Joh TH (1998). Localization of GTP cyclohydrolase in monoaminergic but not nitric oxide-producing cells. Synapse 28: 140–153.

Katagiri N, Chida S, Abe K, Nojima H, Kitabatake M, Hoshi K *et al*. (2010). Preventative effects of 1,3-dimethyl- and 1,3-dimethyl-N-propargyl-1,2,3,4-tetrahydroisoquinoline on MPTP-induced Parkinson's disease-like symptoms in mice. Brain Res 1321: 133–142.

Kim EM, Hwang O (2011). Role of matrix metalloproteinase-3 in neurodegeneration. J Neurochem 116: 22–32.

Kim EM, Shin EJ, Choi JH, Son HJ, Park IS, Joh TH *et al*. (2010a). Matrix metalloproteinase-3 is increased and participates in neuronal apoptotic signaling downstream of caspase-12 during endoplasmic reticulum stress. J Biol Chem 285: 16444–16452.

Kim ST, Choi JH, Chang JW, Kim SW, Hwang O (2005a). Immobilization stress causes increases in tetrahydrobiopterin, dopamine, and neuromelanin and oxidative damage in the nigrostriatal system. J Neurochem 95: 89–98.

Kim ST, Son HJ, Choi JH, Ji IJ, Hwang O (2010b). Vertical grid test and modified horizontal grid test are sensitive methods for evaluating motor dysfunctions in the MPTP mouse model of Parkinson's disease. Brain Res 1306: 176–183.

Kim YS, Kim SS, Cho JJ, Choi DH, Hwang O, Shin DH *et al*. (2005b). Matrix metalloproteinase-3: a novel signaling proteinase from apoptotic neuronal cells that activates microglia. J Neurosci 25: 3701–3711.

Kim YS, Choi DH, Block ML, Lorenzl S, Yang L, Kim YJ *et al*. (2007). A pivotal role of matrix metalloproteinase-3 activity in dopaminergic neuronal degeneration via microglial activation. FASEB J 21: 179–187.

Kotake Y, Taguchi R, Okuda K, Sekiya Y, Tasaki Y, Hirobe M *et al*. (2005). Neuroprotective effect of 1-methyl-1,2,3,4-tetrahydroisoquinoline on cultured rat mesencephalic neurons in the presence or absence of various neurotoxins. Brain Res 1033: 143–150.

Kurkowska-Jastrzebska I, Wronska A, Kohutnicka M, Czlonkowski A, Czlonkowska A (1999). The inflammatory reaction following 1-methyl-4-phenyl-1,2,3,6-tetrahydropyridine intoxication in mouse. Exp Neurol 156: 50–61.

Lee SJ, Oh SJ, Chi DY, Kang SH, Kil HS, Kim JS *et al.* (2007a). One-step high-radiochemical-yield synthesis of [^{18}F]FP-CIT using a protic solvent system. Nucl Med Biol 34: 345–351.

Lee SY, Moon Y, Choi DH, Choi JH, Hwang O (2007b). Particular vulnerability of rat mesencephalic dopaminergic neurons to tetrahydrobiopterin: relevance to Parkinson's disease. Neurobiol Dis 25: 112–120.

Lorenc-Koci E, Smiałowska M, Antkiewicz-Michaluk L, Gołembiowska K, Bajkowska M, Wolfarth S (2000). Effect of acute and chronic administration of 1,2,3,4-tetrahydroisoquinoline on muscle tone, metabolism of dopamine in the striatum and tyrosine hydroxylase immunocytochemistry in the substantia nigra, in rats. Neuroscience 95: 1049–1059.

Mun-Bryce S, Lukes A, Wallace J, Lukes-Marx M, Rosenberg GA (2002). Stromelysin-1 and gelatinase A are upregulated before TNF-alpha in LPS-stimulated neuroinflammation. Brain Res 933: 42–49.

Muralikrishnan D, Mohanakumar KP (1998). Neuroprotection by bromocriptine against 1-methyl-4-phenyl-1,2,3,6-tetrahydropyridine-induced neurotoxicity in mice. FASEB J 12: 905–912.

Nagatsu T (1997). Isoquinoline neurotoxins in the brain and Parkinson's disease. Neurosci Res 29: 99–111.

NINDS NET-PD Investigators (2008). A pilot clinical trial of creatine and minocycline in early Parkinson disease: 18-month results. Clin Neuropharmacol 31: 141–150.

Nuttall RK, Silva C, Hader W, Bar-Or A, Patel KD, Edwards DR *et al.* (2007). Metalloproteinases are enriched in microglia compared with leukocytes and they regulate cytokine levels in activated microglia. Glia 55: 516–526.

Okuda K, Kotake Y, Ohta S (2006). Parkinsonism-preventing activity of 1-methyl-1,2,3,4-tetrahydroisoquinoline derivatives in C57BL mouse in vivo. Biol Pharm Bull 29: 1401–1403.

Pardridge WM (2005). The blood-brain barrier: bottleneck in brain drug development. NeuroRx 2: 13–14.

Recanatini M, Poluzzi E, Masetti M, Cavalli A, De Ponti F (2005). QT prolongation through hERG K(+) channel blockade: current knowledge and strategies for the early prediction during drug development. Med Res Rev 25: 133–166.

Rodrigues AD (1997). Preclinical drug metabolism in the age of high-throughput screening: an industrial perspective. Pharm Res 14: 1504–1510.

Sairam K, Saravanan KS, Banerjee R, Mohanakumar KP (2003). Non-steroidal anti-inflammatory drug sodium salicylate, but not diclofenac or celecoxib, protects against 1-methyl-4-phenyl pyridinium-induced dopaminergic neurotoxicity in rats. Brain Res 966: 245–252.

Schweigert N, Zehnder AJ, Eggen RI (2001). Chemical properties of catechols and their molecular modes of toxic action in cells, from microorganisms to mammals. Environ Microbiol 3: 81–91.

Seo JW, Srisook E, Son HJ, Hwang O, Cha YN, Chi DY (2005). Syntheses of NAMDA derivatives inhibiting NO production in BV-2 cells stimulated with lipopolysaccharide. Bioorg Med Chem Lett 15: 3369–3373.

Seo JW, Srisook E, Son HJ, Hwang O, Cha YN, Chi DY (2008). Syntheses of tetrahydroisoquinoline derivatives that inhibit NO production in activated BV-2 microglial cells. Eur J Med Chem 43: 1160–1170.

Sierra A, Gottfried-Blackmore AC, McEwen BS, Bulloch K (2007). Microglia derived from aging mice exhibit an altered inflammatory profile. Glia 55: 412–424.

Staudacher I, Schweizer PA, Katus HA, Thomas D (2010). hERG: protein trafficking and potential for therapy and drug side effects. Curr Opin Drug Discov Devel 13: 23–30.

Suri C, Fung BP, Tischler AS, Chikaraishi DM (1993). Catecholaminergic cell lines from the brain and adrenal glands of tyrosine hydroxylase-SV40 T antigen transgenic mice. J Neurosci 13: 1280–1291.

Tang Y, Donnelly KC, Tiffany-Castiglioni E, Mumtaz MM (2003). Neurotoxicity of polycyclic aromatic hydrocarbons and simple chemical mixtures. J Toxicol Environ Health A 66: 919–940.

Tansey MG, McCoy MK, Frank-Cannon TC (2007). Neuroinflammatory mechanisms in Parkinson's disease: potential environmental triggers, pathways, and targets for early therapeutic intervention. Exp Neurol 208: 1–25.

Tasaki Y, Makino Y, Ohta S, Hirobe M (1991). 1-Methyl-1,2,3,4-tetrahydroisoquinoline, decreasing in 1-methyl-4-phenyl-1,2,3,6-tetrahydropyridine-treated mouse, prevents parkinsonism-like behavior abnormalities. J Neurochem 57: 1940–1943.

Tatton WG, Chalmers-Redman R, Brown D, Tatton N (2003). Apoptosis in Parkinson's disease: signals for neuronal degradation. Ann Neurol 53 (Suppl. 3): S61–S70; discussion S70–72.

Tejima E, Guo S, Murata Y, Arai K, Lok J, van Leyen K *et al.* (2009). Neuroprotective effects of overexpressing tissue inhibitor of metalloproteinase TIMP-1. J Neurotrauma 26: 1935–1941.

Thomas M, Le WD, Jankovic J (2003). Minocycline and other tetracycline derivatives: a neuroprotective strategy in Parkinson's disease and Huntington's disease. Clin Neuropharmacol 26: 18–23.

Tikka T, Fiebich BL, Goldsteins G, Keinanen R, Koistinaho J (2001). Minocycline, a tetracycline derivative, is neuroprotective against excitotoxicity by inhibiting activation and proliferation of microglia. J Neurosci 21: 2580–2588.

Venkatesh PR, Goh E, Zeng P, New LS, Xin L, Pasha MK *et al.* (2007). In vitro phase I P450 metabolism, permeability and pharmacokinetics of SB639, a novel histone deacetylase inhibitor in preclinical species. Biol Pharm Bull 30: 1021–1024.

Visse R, Nagase H (2003). Matrix metalloproteinases and tissue inhibitors of metalloproteinases: structure, function, and biochemistry. Circ Res 92: 827–839.

Wienkers LC, Heath TG (2005). Predicting in vivo drug interactions from in vitro drug discovery data. Nat Rev Drug Discov 4: 825–833.

Woo MS, Park JS, Choi IY, Kim WK, Kim HS (2008). Inhibition of MMP-3 or -9 suppresses lipopolysaccharide-induced expression of proinflammatory cytokines and iNOS in microglia. J Neurochem 106: 770–780.

Wu DC, Jackson-Lewis V, Vila M, Tieu K, Teismann P, Vadseth C *et al.* (2002). Blockade of microglial activation is neuroprotective in the 1-methyl-4-phenyl-1,2,3,6-tetrahydropyridine mouse model of Parkinson disease. J Neurosci 22: 1763–1771.

Zhou Z, Gong Q, Ye B, Fan Z, Makielski JC, Robertson GA *et al.* (1998). Properties of hERG channels stably expressed in HEK293 cells studied at physiological temperature. Biophys J 74: 230–241.